Received October 30, 2020, accepted November 8, 2020, date of publication November 11, 2020,
date of current version November 20, 2020.

Digital Object Identifier 10.1109/ACCESS.2020.3037352

Tracking Control of Magnetic Levitation System Using Model-Free RBF Neural Network Design

WANG YANG[1], FANWEI MENG[1], SHENGYA MENG[1], SUN MAN[1], AND AIPING PANG[2]
[1]School of Control Engineering, Northeastern University at Qinhuangdao, Qinhuangdao 066004, China
[2]College of Electrical Engineering, Guizhou University, Guiyang 550025, China

Corresponding author: Sun Man (sunman@neuq.edu.cn)

This work was supported in part by the Fundamental Research Funds for the Central Universities under Grant N182304010, and in part by the Natural Science Foundation of Hebei Province under Grant F2019501012.

ABSTRACT This paper focuses on the tracking control problem of Magnetic Levitation System (MLS). MLS is highly unstable nonlinear system, in the process of operation, MLS needs to have strong robustness and anti-interference ability. Due to disturbance and parameter uncertainties in MLS, it is complex to obtain the exact dynamics of MLS, and it is difficult to design a suitable controller. The dynamic equation of the system is established by Lagrange equation, and then we propose an adaptive Sliding Mode Control (SMC) based on Radial Basis Function Neural Network (RBFNN). Because of the parameter uncertainties and disturbance in MLS, RBFNN is used to approximate the unknown dynamics in MLS. The stability of the closed-loop system is strictly proved by using the Lyapunov stability theory, which can achieve the uniform ultimate boundedness (UUB) of the signals of the closed-loop MLS. MATLAB environment is used to verify the performance of the proposed controller. Considering disturbance, parameter change, or unmodeled dynamics in MLS, proposed controller is compared with other nonlinear controllers, simulation results verify the effectiveness of the proposed approach.

INDEX TERMS Tracking, magnetic levitation system (MLS), neural network, Lyapunov stability.

I. INTRODUCTION

MLS is a highly unstable nonlinear system with single input and single output (SISO) [1]–[5]. The basic principle of magnetic levitation system is to balance the gravity of electromagnet through the electromagnetic force generated by current. The mathematical model is represented by the third-order nonlinear differential equation. The main purpose of MLS control is to make the system have strong tracking and anti-interference ability. MLS has the advantages of low energy consumption, no friction and so on. It has been widely used in engineering and education, such as magnetic levitation bearing [6], magnetic levitation train [7]–[9], magnetic levitation wind turbines [10], etc. The controller design is very important for engineering application, and the control of MLS is an important and attractive research direction in the control field.

In recent years, the problem of tracking control has been widely studied [11], [12], for instance, a fuzzy tracking controller is applied to completely non-affine uncertain switched pure-feedback nonlinear systems [13]. Reference [14] considers the problem of fuzzy output-feedback tracking control for switched stochastic nonlinear systems in pure-feedback form. Reference [15] considers the quantized static output feedback dissipative tracking control problem for a class of discrete-time nonlinear networked systems based on Takagi-Sugeno fuzzy model approach. In order to improve the tracking ability of MLS, a variety of control methods have been applied to the control of MLS. Parameter estimation and generalized proportional integral control (GPIC) are proposed [16], and the exponential asymptotic stability of the system is guaranteed. Under the premise of nonlinear model, a hybrid control based on disturbance observer is designed to cancel the mismatched disturbance in the system and improves the anti-interference ability of the system [17]. A controller based on feedback linearization model is developed, and the control effect is better than the traditional cascade control of voltage and current [18]. The exponential tracking problem of MLS is studied under the condition of parameter uncertainty and external disturbance [19]. A Fractional Order PID controller is proposed, and the parameters of the controller are optimized by ant colony algorithm [20]. An Integral Backstepping controller is used to realize the suspension control, and the steady-state error of the

The associate editor coordinating the review of this manuscript and approving it for publication was Manuel Rosa-Zurera.

system is reduced [21]. According to the parameter estimation observer, the problem of sensorless state observation of MLS is solved [22]. The chattering in traditional sliding mode control is eliminated by using supertwisting algorithm, and the asymptotic stability of tracking error is guaranteed in the presence of time-varying uncertain parameters and external disturbances [23]. Considering the nonlinear characteristics of the nonlinear MLS and the actual working environment, if the uncertainty or disturbance is large, the performance of MLS will deteriorate rapidly, so it is necessary to design a more robust controller. RBFNN Sliding Mode Control (RBFNNSMC) is proposed to deal with the unknown dynamics of MLS. Due to the universal approximation ability of neural networks, it is usually used to approximate unknown functions in control systems [24]. A RBFNN is directly used to design controller to deal with disturbance and parameters change in coupled motor drives [25]. Fuzzy wavelet neural network is proposed to improve tracking control accuracy of manipulator [26]. Nonlinear dynamical model of friction is approximated by neural networks [27]. In order to deal with the main issues including the communication time delay, various nonlinearities and uncertainties, an RBF adaptive controller is addressed for nonlinear bilateral teleoperation manipulators [28]. Reference [29] proposes a force sensorless control scheme based on neural network for interaction between robot manipulators and human arms in physical collision.

The main contributions of this paper include the following. An affine nonlinear model of MLS is established by Lagrange equation. In order to reduce the complexity of the model, the magnitude of magnetic flux is selected as the independent variable. The conventional methods need to use the precise mathematical model of MLS, but the precise model is not easy to establish. The conventional methods are sensitive to the system parameter change and disturbance. The proposed method does not need to know the precise model of the system, RBFNN are used to approximate the unknown dynamics in MLS. The proposed controller guarantees that the signals of the closed-loop MLS are UUB. Parameter change, disturbance, or unmodeled dynamics will be used to analyze the robustness and anti-interference ability of the proposed controller later.

The rest of this paper is arranged as follows: Section II establishes the affine nonlinear model of MLS by using Lagrange equation, in order to reduce the complexity of the model, the magnitude of magnetic flux is selected as variable. the input-output feedback linearization controller is designed in Section III. RBFNNSMC is proposed and system's stability is proved in Section IV. Section V analyzes the simulation results of closed-loop MLS. Section VI is the conclusion.

II. MATHEMATICAL MODELING OF MLS BASED ON LAGRANGE EQUATION

Generally, Newton's law and Kirchhoff's law are used to establish the nonlinear model of MLS. Considering the advantages of Lagrange equation modeling, that is, only considering the energy of the whole system, and selecting reasonable generalized coordinates for MLS, modeling the system from the angle of energy can reduce the difficulty of the problem, and quickly get the nonlinear differential equation of the system. A simple single degree of freedom MLS block diagram is shown in Fig. 1. table 1 shows the parameters of Fig. 1.

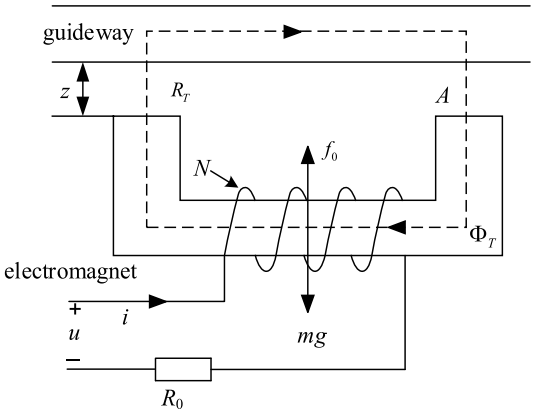

FIGURE 1. MLS model.

TABLE 1. Symbols of MLS in Fig. 1.

Symbol	Meaning
z	air gap between magnet and rail
R_T	air gap resistance
A	magnetic pole area
N	numbers of coil
f	electromagnetic force
Φ_T	main flux
m	mass of suspension magnet
g	acceleration of gravity
i	current
u	voltage
R_0	coil resistance

Assumption 1: The magnetic resistance of the magnetic circuit formed by electromagnet and guide rail is mainly concentrated in the air gap between them.

Assumption 2: Ignore flux leakage.

It can be seen from Fig. 1 that the input is voltage, and the current in the coil is used to generate electromagnetic force. The electromagnetic force keeps the controlled plant suspended at a given position. By changing the voltage, different electromagnetic forces are generated to make the system suspend in different positions. The main purpose of control is to make the system have strong tracking ability and robustness.

It can be obtained from Assumption 1

$$R_T = \frac{2z}{\mu_0 A} \tag{1}$$

From Assumption 2, we get magnitude of magnetic flux λ

$$\lambda = N\Phi_T = L_\mu(z)i \tag{2}$$

where the coil winding inductance

$$L_\mu(z) = \frac{N\Phi_T}{i} = \frac{N}{i} * \frac{Ni}{R_T} = \frac{\mu_0 N^2 A}{2z} \tag{3}$$

Electromagnetic energy of the system is

$$E(z,i) = \frac{1}{2}L_\mu(z)i^2 \tag{4}$$

From (4), we get f_0

$$f_0(z,i) = -\frac{\partial E}{\partial z} = \frac{\mu_0 N^2 A}{4}\left[\frac{i}{z}\right]^2 \tag{5}$$

Since the Lagrange equation is used in the modeling process, the following will briefly introduce the Lagrange equation. For an energy dissipative system with degree of freedom n, the Lagrange equation with dissipation function is [30]

$$\frac{\mathrm{d}}{\mathrm{d}t}\left(\frac{\partial L}{\partial \dot{r}_j}\right) - \frac{\partial L}{\partial r_j} = -\frac{\partial G}{\partial \dot{r}_j} + Q_j \quad j = 1, \ldots.., n \tag{6}$$

where L is the Lagrange function, r and $\dot{r}$ are the generalized coordinates and their derivatives respectively, G is the dissipation function of the system, and Q_j is a generalized force that is non-potential force except the dissipative force.

Take the MLS as the research plant, According to (6), $r_1 = z$ and $r_2 = q$ are the generalized coordinate and $\dot{z}$ and $\dot{q} = i$ are corresponding derivative.

The kinetic energy of MLS can be written as

$$T = \frac{1}{2}m\dot{z}^2 + E(z,i) \tag{7}$$

The potential energy of MLS can be written as

$$V_0 = -mgz \tag{8}$$

From (7)-(8), we get

$$L = T - V_0 = \frac{1}{2}m\dot{z}^2 + E(z,i) + mgz \tag{9}$$

The energy dissipation function in MLS is

$$G = \frac{1}{2}R_0 i^2 \tag{10}$$

For generalized coordinates r_1 and r_2, we have

$$Q_1 = 0, \quad Q_2 = u \tag{11}$$

Substituting (9)-(11) into (6), we get (12)

$$\begin{cases} \dfrac{\mathrm{d}}{\mathrm{d}t}\left(\dfrac{\partial L}{\partial \dot{z}}\right) - \dfrac{\partial L}{\partial z} = -\dfrac{\partial G}{\partial \dot{z}} + Q_1 \\ \dfrac{\mathrm{d}}{\mathrm{d}t}\left(\dfrac{\partial L}{\partial \dot{q}}\right) - \dfrac{\partial L}{\partial q} = -\dfrac{\partial G}{\partial \dot{q}} + Q_2 \end{cases} \tag{12}$$

Equation (12) can be written as

$$\begin{cases} \ddot{z} = -\dfrac{ki^2}{4mz^2} + g \\ \dot{i} = \dfrac{2z}{k}(-R_0 i + u) + \dfrac{i}{z}\dot{z} \end{cases} \tag{13}$$

Combining (2)-(3) and (12)-(13), we have

$$\begin{cases} \ddot{z} = a\lambda^2 + g \\ \dot{\lambda} = b\lambda z + u \end{cases} \tag{14}$$

where $a = -\frac{1}{km}$, $b = -\frac{2R_0}{k}$, k is constant, $k = \mu_0 A N^2$, μ_0 is permeability of vacuum.

Defining state variables

$$\boldsymbol{x} = [x_1, x_2, x_3]^{\mathrm{T}} = [z, \dot{z}, \lambda]^{\mathrm{T}} \tag{15}$$

Remark 1: According to (12)-(15), selecting λ instead of i as variable reduces the complexity of the model [31] simplifies the complicated mathematical derivation in the process of controller design. In (14), λ^2 and λz are nonlinear function, it shows that MLS is nonlinear system.

III. FEEDBACK LINEARIZATION CONTROL OF MLS

The SISO nonlinear system in the form of (16) is considered.

$$y^{(n)} = \chi\left(y^{(n-1)}, y^{(n-2)}, \ldots, \dot{y}, y, u\right) \tag{16}$$

where y is the system output, u is the control variable, and χ is continuous function.

The feedback linearization control law can be easily obtained by (16), and the expected closed-loop system is shown in (17)

$$y^{(n)} = k_0\left(x_{\mathrm{r}} - y\right) - k_1\dot{y} - \cdots - k_{n-1}y^{(n-1)} \tag{17}$$

where $k_0, k_1, \ldots, k_{n-1}$ is the expected coefficient, x_r is reference input.

According to (16)-(17), we have

$$\chi\left(y^{(n-1)}, y^{(n-2)}, \ldots, \dot{y}, y, u\right) = k_0\left(y_{\mathrm{r}} - y\right) - k_1\dot{y} - \cdots - k_{n-1}y^{(n-1)} \tag{18}$$

From (18), we get

$$u = \psi\left(y^{(n-1)}, y^{(n-2)}, \ldots, \dot{y}, y - y_{\mathrm{r}}\right)$$

For the MLS in this paper, we have

$$y = x_1 \tag{19}$$

Taking time derivative of (19)

$$\dot{y} = \dot{x}_1 = x_2 \tag{20}$$

Taking time derivative of (20)

$$\ddot{y} = \dot{x}_2 = \ddot{x}_1 = ax_3^2 + g \tag{21}$$

Taking time derivative of (21)

$$y = \dddot{x}_2 = x_1 = 2ax_3(bx_3x_1 + u) = f(x) + l(x)u \tag{22}$$

where $f(x) = 2abx_1x_3^2$, $l(x) = 2ax_3$, The control u appears on the right side of (22). Design the ideal closed-loop differential equation as shown in (23)

$$\dddot{y} = k_0\left(x_{\mathrm{r}} - y\right) - k_1\dot{y} - k_1\ddot{y} \tag{23}$$

TABLE 2. Controller parameters corresponding to different T_s.

T_s	$[k_0, k_1, k_2]$	curve in Fig. 3
0.2	[27000, 2700, 90]	z_1
0.3	[8000, 1200, 60] ,	z_2
0.4	[3375, 675, 45]	z_3

Defining error e

$$e = x_r - x_1 \tag{24}$$

The basic objective of control is to ensure that the MLS can track reference input within limited time t_0, i.e., $e \to 0$, as $t \to t_0$.

From (22)-(24), we have

$$\begin{aligned} f(x) + l(x)u &= k_0 (y_r - y) - k_1\dot{y} - k_2\ddot{y} \\ u &= \frac{1}{l}(k_0 (y_r - y) - k_1\dot{y} - k_2\ddot{y} - f) \\ &= \frac{1}{l}(-f + \sum_{i=0}^{2} k_i e^{(i)}) \end{aligned} \tag{25}$$

where $e^{(i)} = \frac{d^{(i)}e}{dt^{(i)}}$. The feedback linearization control structure diagram of MLS is shown in Fig. 2.

Feedback linearization is generally combined with the classical pole placement method to design the controller. According to the pole assignment method, the settling time is defined as T_s, and $\beta = 6/T_s$, controller satisfies $[k_0, k_1, k_2] = [\beta^3, 3\beta^2, 3\beta]$, Different T_s corresponding controllers are shown in table 2.

In Fig. 3, z_r is the reference input. It can be seen from table 2 that when $T_s = 0.2$, the coefficient of the controller is the largest, the initial overshoot of the system response is the smallest; when $T_s = 0.4$, the coefficient of the controller is the smallest, the corresponding initial overshoot of the system response is the largest. Assuming that the system has a change in model coefficient, the specific change is shown in (26). The curve z_1 is most affected by the change of parameters, and the maximum change is 0.0016m. Curve z_3 is the least affected by parameter change, and its maximum variation is 0.0005m. Although the decrease of T_s can reduce the initial overshoot and the stronger the anti-interference ability, but we can't set the settling time of the system to zero, which is not in line with the actual situation. In the process of feedback linearization control design, the accurate model of the system is needed, which can't deal with the problems such as unknown dynamics and parameters change. In the next section, RBFNN combined with SMC is introduced to solve the control problems under the condition of unknown dynamics or parameters change.

$$b = \begin{cases} 0.85b_0 & 3 \le t \le 3.2 \\ b_0 & \text{else} \end{cases} \tag{26}$$

where b_0 is the nominal value of the coefficient b.

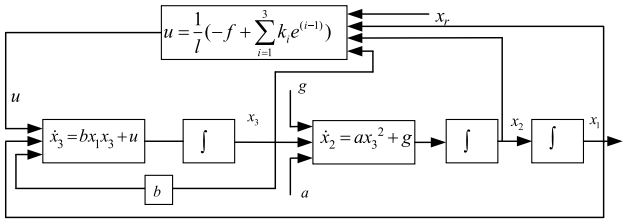

FIGURE 2. Feedback linearization control structure block diagram of MLS.

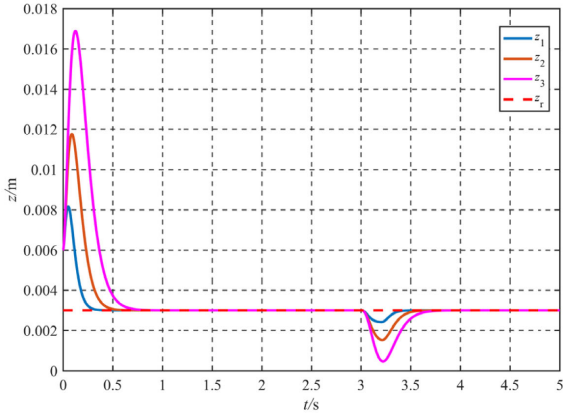

FIGURE 3. The response of MLS with different T_s.

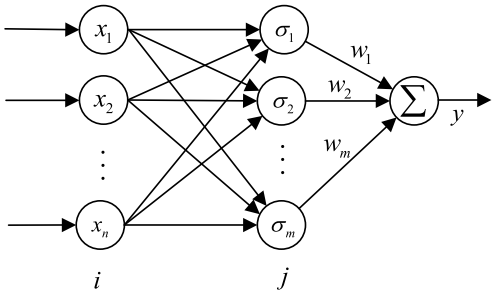

FIGURE 4. Structure of RBFNN.

IV. DESIGN AND STABILITY ANALYSIS OF RBFNN SLIDING MODE TRACKING CONTROLLER

In this Section, firstly, RBFNN is introduced, and then RBFNNSMC is designed for MLS with unknown dynamics.

A. RADIAL BASIS FUNCTION NEURAL NETWORK

RBFNN can approximate any continuous function with arbitrary precision [24], Fig. 4 describes the single implicit layer structure of RBFNN, SMC is simple and robust, and it is widely used in control system, especially in deterministic system which can establish accurate mathematical model [32]. In this paper, the RBFNNSMC is designed considering the advantages of neural network and SMC.

Because of the disturbance and parameters change in the system, $f(\boldsymbol{x})$ and $l(\boldsymbol{x})$ cannot be accurately obtained. Considering that $f(\boldsymbol{x})$ and $l(\boldsymbol{x})$ are unknown in MLS (22), RBFNN can be used to approximate $f(\boldsymbol{x})$ and $l(\boldsymbol{x})$ under the condition of satisfying assumption 3 and 4, as shown in (28). Although SMC can deal with the disturbance and uncertainty in the

feedback system, it can not provide a satisfactory scheme when system's dynamics is unknown. When the system dynamics is unknown, RBFNNSMC method is proposed. The stability proof based on Lyapunov theory is provided. The weight coefficient of neural network is obtained by using the adaptive law of online learning to ensure the tracking ability of MLS.

where σ_j is the radial basis function, as shown in (27)

$$\sigma_j = \exp\left(\frac{-(\boldsymbol{x}-\boldsymbol{\mu}_j)^{\mathrm{T}}(\boldsymbol{x}-\boldsymbol{\mu}_j)}{2b_j^2}\right), \quad j = 1, 2, \ldots m \tag{27}$$

Assumption 3: $\boldsymbol{x}$ is bounded, $f(\boldsymbol{x})$ and $l(\boldsymbol{x})$ are smooth functions, and $|f(\boldsymbol{x})| \leq f_{\max}$, $|l(\boldsymbol{x})| \leq l_{\max}$, $\forall \boldsymbol{x} \in U_1$.

Assumption 4: There are optimal weights $\boldsymbol{W}^*$ and $\boldsymbol{N}^*$, satisfying

$$\begin{aligned}\boldsymbol{W}^* &= \arg \underbrace{\min}_{\boldsymbol{W}\in U_2}\{\underbrace{\sup}_{x\in U_1}\left\|\boldsymbol{W}^{\mathrm{T}}\boldsymbol{\sigma}_f(\boldsymbol{x}) - f\right\|\}\\ \boldsymbol{N}^* &= \arg \underbrace{\min}_{\boldsymbol{N}\in U_3}\{\underbrace{\sup}_{x\in U_1}\left\|\boldsymbol{N}^{\mathrm{T}}\boldsymbol{\sigma}_l(\boldsymbol{x}) - l\right\|\}\end{aligned}$$

where U_1, U_2, U_3 are bounded closed sets. f, l is short for $f(\boldsymbol{x}), l(\boldsymbol{x})$.

$$\begin{aligned}f(\boldsymbol{x}) &= \boldsymbol{W}^{*\mathrm{T}}\boldsymbol{\sigma}_f(\boldsymbol{x}) + \varepsilon_f(\boldsymbol{x})\\ l(\boldsymbol{x}) &= \boldsymbol{N}^{*\mathrm{T}}\boldsymbol{\sigma}_l(\boldsymbol{x}) + \varepsilon_l(\boldsymbol{x})\end{aligned} \tag{28}$$

where x is the input vector of the neural network, $\boldsymbol{\sigma}(\boldsymbol{x}) = [\sigma_1(\boldsymbol{x}), \sigma_2(\boldsymbol{x}), \cdots, \sigma_m(\boldsymbol{x})]^{\mathrm{T}}$, and ε is the approximation error of RBFNN, $|\varepsilon_f| \leq \varepsilon_{\max}$, $|\varepsilon_l| \leq \varepsilon_{\max}$.

B. CONTROLLER DESIGN AND STABILITY PROOF OF CLOSED-LOOP SYSTEM

Suppose that f and l are known in (22), define sliding mode function s

$$s = [c_1 \quad c_2 \quad 1][e \quad \dot{e} \quad \ddot{e}]^{\mathrm{T}} \tag{29}$$

where $c_i > 0$, $i = 1, 2$, And the polynomial $\lambda^2 + c_2\lambda + c_1$ is Hurwitz, so $e \to 0$ as $s \to 0$.

From (29) and (22), we have

$$\begin{aligned}\dot{s} &= c_1\dot{e} + c_2\ddot{e} + \dddot{e}\\ &= c_1(\dot{x}_r - \dot{x}_1) + c_2(\ddot{x}_r - \ddot{x}_1) + (\dddot{x}_r - \dddot{x}_1)\\ &= -f - lu + \dddot{x}_r + c_1\dot{e} + c_2\ddot{e}\end{aligned} \tag{30}$$

where

$$u = \frac{1}{l}(-f + \dddot{x}_r + c_1\dot{e} + c_2\ddot{e} + k_\sigma s) \tag{31}$$

Defining Lyapunov functions V

$$V = \frac{1}{2}s^2 \tag{32}$$

From (29) - (32), it can be obtained

$$\dot{V} = -k_\sigma s^2 \leq 0$$

Therefore, MLS is stable.

Considering that f and l are unknown in system (22), sliding mode controller u and neural network parameter vector $\hat{\boldsymbol{N}}$ and $\hat{\boldsymbol{W}}$ is designed, makes $e \to 0$ as $s \to 0$.

Theorem 1: Considering that f and l are unknown in system (22), and satisfy Assumption 3-4, the controller is (33), the adaptive law is (34), then the closed-loop system is UUB.

$$u = \frac{1}{\hat{l}}(-\hat{f} + \dddot{x}_r + c_1\dot{e} + c_2\ddot{e} + k_\sigma s + \tau\mathrm{sgn}(s)) \tag{33}$$

where

$$\mathrm{sgn}(s) = \begin{cases}1 & s > 0\\ 0 & s = 0\\ -1 & s < 0\end{cases}$$

$$\begin{cases}\dot{\hat{\boldsymbol{W}}} = -\xi(s\sigma_f + \gamma\hat{\boldsymbol{W}})\\ \dot{\hat{\boldsymbol{N}}} = -\delta(s\sigma_l u + \varsigma\hat{\boldsymbol{N}})\end{cases} \tag{34}$$

where

$$\hat{f} = \hat{\boldsymbol{W}}^{\mathrm{T}}\boldsymbol{\sigma}_f, \quad \hat{l} = \hat{\boldsymbol{N}}^{\mathrm{T}}\boldsymbol{\sigma}_l \tag{35}$$

where $\hat{f}$ and $\hat{l}$ are estimates of f and l, respectively, satisfying $\tilde{\boldsymbol{W}} = \hat{\boldsymbol{W}} - \boldsymbol{W}^*$, $\tilde{\boldsymbol{N}} = \hat{\boldsymbol{N}} - \boldsymbol{N}^*$.

Remark 2: In order to avoid the influence of RBFNN on the system stability, a robust term $\tau\mathrm{sgn}(s)$ is added. ξ and δ are positive constant, which determines the convergence rate of $\hat{\boldsymbol{W}}$ and $\hat{\boldsymbol{N}}$, γ and ς are small positive constants, which are mainly used to reduce the error of RBFNN approximation, and can also avoid the influence of excessive weight drift on system performance. The scheme of RBFNNSMC is shown in Fig. 5.

Proof: the Lyapunov function chosen is

$$V = \frac{1}{2}s^2 + \frac{1}{2}\xi^{-1}\tilde{\boldsymbol{W}}^T\tilde{\boldsymbol{W}} + \frac{1}{2}\delta^{-1}\tilde{\boldsymbol{N}}^{\mathrm{T}}\tilde{\boldsymbol{N}} \tag{36}$$

The time derivative of (36) is written as

$$\begin{aligned}\dot{V} &= s\dot{s} + \xi^{-1}\tilde{\boldsymbol{W}}^{\mathrm{T}}\dot{\hat{\boldsymbol{W}}} + \delta^{-1}\tilde{\boldsymbol{N}}^{\mathrm{T}}\dot{\hat{\boldsymbol{N}}}\\ &= s(-\dddot{x}_1 + \dddot{x}_r + c_1\dot{e} + c_2\ddot{e}) + \xi^{-1}\tilde{\boldsymbol{W}}^{\mathrm{T}}\dot{\hat{\boldsymbol{W}}} + \delta^{-1}\tilde{\boldsymbol{N}}^{\mathrm{T}}\dot{\hat{\boldsymbol{N}}}\\ &= s(-f - \hat{l}u + (\hat{l} - l)u + \dddot{x}_r + c_1\dot{e} + c_2\ddot{e})\\ &\quad + \xi^{-1}\tilde{\boldsymbol{W}}^{\mathrm{T}}\dot{\hat{\boldsymbol{W}}} + \delta^{-1}\tilde{\boldsymbol{N}}^{\mathrm{T}}\dot{\hat{\boldsymbol{N}}}\end{aligned} \tag{37}$$

From (33), (37) can be rewritten as

$$\begin{aligned}\dot{V} &= s(-f - \frac{\hat{l}}{\hat{l}}(-\hat{f} + \dddot{x}_r + c_1\dot{e} + c_2\ddot{e} + k_\sigma s\\ &\quad + \ldots\tau\mathrm{sgn}(s)) + (\hat{l} - l)u + \dddot{x}_r + c_1\dot{e} + c_2\ddot{e})\\ &\quad + \ldots\xi^{-1}\tilde{\boldsymbol{W}}^{\mathrm{T}}\dot{\hat{\boldsymbol{W}}} + \delta^{-1}\tilde{\boldsymbol{N}}^{\mathrm{T}}\dot{\hat{\boldsymbol{N}}}\\ &= s(\hat{f} - f + (\hat{l} - l)u - k_\sigma s - \tau\mathrm{sgn}(s))\\ &\quad + \ldots\xi^{-1}\tilde{\boldsymbol{W}}^{\mathrm{T}}\dot{\hat{\boldsymbol{W}}} + \delta^{-1}\tilde{\boldsymbol{N}}^{\mathrm{T}}\dot{\hat{\boldsymbol{N}}}\end{aligned} \tag{38}$$

From (29) and (35), (38) can be rearranged as

$$\begin{aligned}\dot{V} &= s(\tilde{\boldsymbol{W}}^{\mathrm{T}}\sigma_f + \varepsilon_f + \tilde{N}^{\mathrm{T}}\sigma_l u + \varepsilon_l u\\ &\quad - \ldots k_\sigma s - \tau\mathrm{sgn}(s)) + \xi^{-1}\tilde{\boldsymbol{W}}^{\mathrm{T}}\dot{\hat{\boldsymbol{W}}} + \delta^{-1}\tilde{\boldsymbol{N}}^{\mathrm{T}}\dot{\hat{\boldsymbol{N}}}\end{aligned}$$

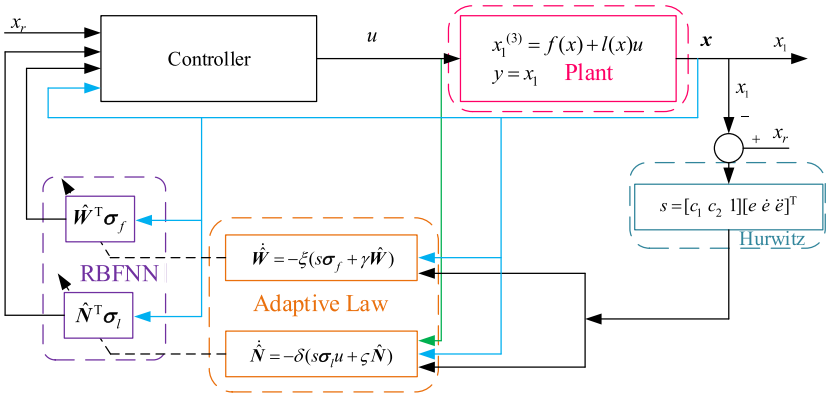

FIGURE 5. Block diagram of RBFNNSMC.

$$= -k_\sigma s^2 + \tilde{W}^T(\xi^{-1}\dot{\hat{W}} + s\sigma_f) + \ldots \tilde{N}^T(\delta^{-1}\dot{\hat{N}} + s\sigma_l u) + (\varepsilon_f + \varepsilon_l u)s - \tau\,|s| \quad (39)$$

Defining $\tau \geq |\varepsilon_f + \varepsilon_l u|$, from (34), (39) can be rearranged as

$$\dot{V} = -k_\sigma s^2 - \gamma\tilde{W}^T\hat{W} - \varsigma\tilde{N}^T\hat{N} \quad (40)$$

with regard to the two coupling terms in (40), there are the following facts.

$$\gamma\tilde{W}^T\hat{W} = \frac{\gamma}{2}(\tilde{W}^T(W^* + \tilde{W}) + (\hat{W} - W^*)^T\hat{W}) \times \gamma\tilde{W}^T\hat{W} = \frac{\gamma}{2}(\tilde{W}^T\tilde{W} + \hat{W}^T\hat{W} - W^{*T}W^*) - \gamma\tilde{W}^T\hat{W} \leq -\frac{\gamma}{2}(\tilde{W}^T\tilde{W} - W^{*T}W^*) \quad (41)$$

Similarly

$$-\varsigma\tilde{N}^T\hat{N} \leq -\frac{\varsigma}{2}\tilde{N}^T\tilde{N} + \frac{\varsigma}{2}N^{*T}N^* \quad (42)$$

Equation (40) can be rewritten as

$$\dot{V} \leq -\alpha V + \eta + \alpha(\frac{1}{2}s^2 + \frac{1}{2\xi}\tilde{W}^T\tilde{W} + \frac{1}{2\delta}N^{*T}N^*) - \eta \ldots - k_\sigma s^2 - \frac{\gamma}{2}(\tilde{W}^T\tilde{W} - W^{*T}W^*) - \frac{\varsigma}{2}(\tilde{N}^T\tilde{N} - N^{*T}N^*) \quad (43)$$

where

$$\eta = \frac{\gamma}{2}W^{*T}W^* + \frac{\varsigma}{2}N^{*T}N^*, \quad 0 < \alpha = 2\min(k_\sigma, \frac{\xi}{2}\gamma, \frac{\delta}{2}\varsigma)$$

Equation (43) can be rearranged as

$$\dot{V} \leq -\alpha V + \eta + (\frac{\alpha}{2} - k_\sigma)s^2 + (\frac{\alpha}{2\xi} - \frac{\gamma}{2})\tilde{W}^T\tilde{W} + \ldots + (\frac{\alpha}{2\delta} - \frac{\varsigma}{2})\tilde{N}^T\tilde{N} - (\eta - \frac{\gamma}{2}W^{*T}W^* - \frac{\varsigma}{2}N^{*T}N^*)$$
$$\dot{V} \leq -\alpha V + \eta \quad (44)$$

Make some mathematical transformations on (44), we have

$$\dot{V} + \alpha V - \eta = \dot{V}\exp(\alpha t) + \alpha V\exp(\alpha t) - \eta\exp(\alpha t) \leq 0$$
$$= \frac{\mathrm{d}}{\mathrm{d}t}(V\exp(\alpha t) - \frac{\eta}{\alpha}\exp(\alpha t)) \leq 0$$
$$= \int_0^t \frac{\mathrm{d}}{\mathrm{d}t}(V\exp(\alpha t) - \frac{\eta}{\alpha}\exp(\alpha t)) \leq 0$$
$$= V\exp(\alpha t) - \frac{\eta}{\alpha}\exp(\alpha t) - V(0) + \frac{\eta}{\alpha} \leq 0 \quad (45)$$

where $\exp(\alpha t)$ is exponential function.

From (45), we have

$$V \leq (V(0) - \frac{\eta}{\alpha})\exp(-\alpha t) + \frac{\eta}{\alpha} \quad (46)$$

From (36) and (46), we have

$$\frac{1}{2}s^2 \leq V(0) + \frac{\eta}{\alpha}$$
$$\|s\| \leq \sqrt{2Y} \quad (47)$$

where $Y = V(0) + \frac{\eta}{\alpha}$.

Similarly

$$\left\|\tilde{W}\right\| \leq \sqrt{2\xi Y}, \quad \left\|\tilde{N}\right\| \leq \sqrt{2\delta Y} \quad (48)$$

From (46)-(48), we can know that $s, \tilde{W}, \tilde{N}$ is bounded and converges to $\Xi_s, \Xi_{\tilde{W}}, \Xi_{\tilde{N}}$ respectively, and the closed-loop MLS is UUB.

where $\Xi_s, \Xi_{\tilde{W}}, \Xi_{\tilde{N}}$ is given as

$$\begin{cases} \Xi_s = \{s \in R|\ \|s\| \leq \sqrt{2Y}\} \\ \Xi_{\tilde{W}} = \{\tilde{W} \in R^n|\ \left\|\tilde{W}\right\| \leq \sqrt{2\xi Y}\} \\ \Xi_{\tilde{N}} = \{\tilde{N} \in R^n|\ \left\|\tilde{N}\right\| \leq \sqrt{2\delta Y}\} \end{cases} \quad (49)$$

Remark 3: Considering that system (22) is mainly composed of (33)-(35), the initial values of these parameters are bounded, and the proposed controller makes the system meet the Lyapunov stability, so $t > 0$, All signals in MLS are still bounded.

TABLE 3. List of parameters in MLS.

Symbol	Value
m	15 kg
R_0	1.1 Ω
g	9.81m/s^2
k	0.001

V. SIMULATION

In order to verify the effectiveness of the proposed controller (namely RBFNNSMC), the simulation model of the proposed controller is built in Simulink [33], [34]. In order to avoid the chattering of the closed-loop MLS near the sliding surface, (50) is used to approximate sgn(s)

$$\text{sgn}(s) = \frac{s}{|s| + \upsilon} \tag{50}$$

where $\upsilon = 0.05$.

To verify the boundedness of f and l,

$$|f(\boldsymbol{x})| = \left|2abx_1x_3^2\right| \leq 734, \quad |l(x)| = |2ax_3| \leq 67$$

where

$$U_1 = \left\{ \begin{matrix} \boldsymbol{x}|0.001 \leq x_1 \leq 0.01, -0.05 \leq x_2 \leq 0.05, \\ 0.001 \leq x_3 \leq 0.5 \end{matrix} \right\}.$$

The values of parameters in MLS are given in table 3. The initial value of air gap is 0.006 m, and the reference value is 0.003 m. The control gain parameters in (33) are designed as $c_1 = 540, c_2 = 47, k_\sigma = 26, \tau = .1$. The input vector of RBFNN is chosen as $\boldsymbol{x} = [x_1, x_2, x_3]^{\mathrm{T}}$, the structure of RBFNN is taken as 3-9-1. $\boldsymbol{\mu}$ and b_j are determined by the actual operating range of x_1, x_2, x_3, the range of $\boldsymbol{\mu}$ is $[-0.012, 0.012] \times [-0.06, 0.06] \times [-0.8, 0.8]$, nine nodes are used in the area of $\boldsymbol{\mu}$, $b_j = 20$. The gain parameters in (34) are selected as $\xi = 300, \delta = 1.5, \gamma = .001, \varsigma = .01$, the weights of RBFNN are initialized between -2 to 2.

In order to analyze the performance of the proposed controller, we compare the proposed controller with SMC and Backstepping control, and compare their response performance index to verify the superiority of the proposed controller. The proposed controller is not compared with linear controller, because MLS is a highly nonlinear unstable system, linear control needs to linearize the nonlinear dynamics of MLS, the dynamics of MLS is modified, and linear control cannot fully reflect the information of MLS. The proposed controller is a nonlinear controller, and SMC and Backstepping control are nonlinear control, so it is compared with SMC and Backstepping control. The tracking performance of RBFNNSMC, SMC and Backstepping control are shown in Fig. 6, The control input of RBFNNSMC, SMC and Backstepping control are shown in Fig. 7, and performance analysis are shown in table 4.

As can be seen from Fig. 6 and table 4, all three controllers can track the reference input in finite time. To be more exact, the proposed controller has the smallest initial

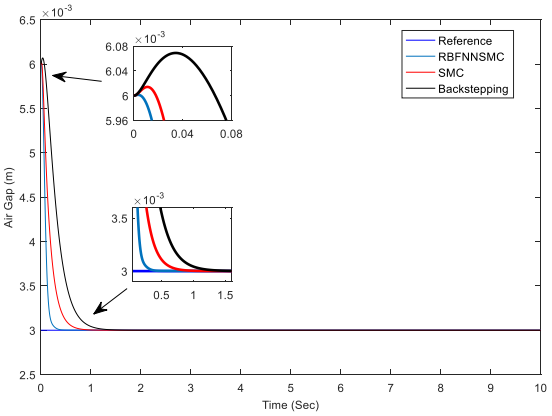

FIGURE 6. Tracking performance of RBFNNSMC, SMC and Backstepping control.

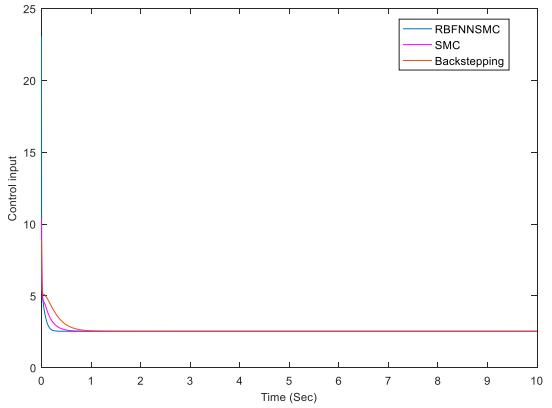

FIGURE 7. Control input of RBFNNSMC, SMC and Backstepping control.

TABLE 4. Performance analysis of three controllers.

Index	RBFNNSMC	Sliding Mode Control	Backstepping Control
Initial overshoot (mm)	0.0015	0.0145	0.069
Steady-state time(s)	0.67	> 1	> 1
Control input (0s-0.003s)	8.03-23.05	8.51-10.37	7.34-8.88
Response speed	quick	middle	slow

overshoot which is 0.0015 mm, SMC's initial overshoot is 0.0145 mm, Backstepping controller has the biggest initial overshoot which is 0.069 mm. The proposed controller can reach steady-state in 0.67 s, and the steady-state time of both SMC and Backstepping control is greater than 1 s. As shown in Fig. 7, the control input of the proposed controller has fast convergence compared with SMC and Backstepping control. To be more precise, from in table 4, in 0 s-.003 s, the control input of the proposed controller is from 23.05 to 8.03, the control input of SMC is from 10.37 to 8.51, and the control input of Backstepping control is from 8.88 to 7.34. On the basis of analysis, we can see that the proposed controller has

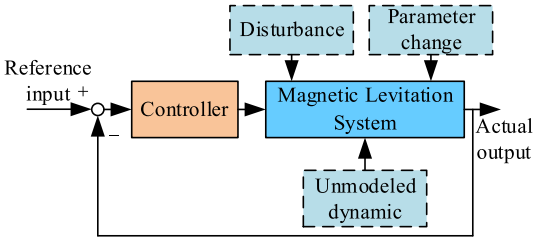

FIGURE 8. Control diagram of MLS in case of Disturbance, Parameter changes or Unmodeled dynamic.

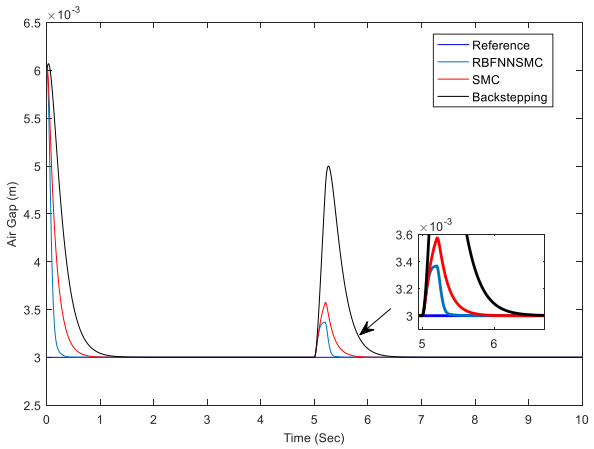

FIGURE 9. Tracking performance of RBFNNSMC, SMC and Backstepping control (in case of Disturbance in short time).

batter tracking capability compared with SMC and Backstepping control. During the operation of MLS, MLS may be influenced by disturbance, parameters change or unmodeled dynamic, and the corresponding control structure diagram is shown in Fig. 8. The anti-interference ability and robustness of the proposed controller will be analyzed later.

For the purpose of analyzing the behavior of the proposed controller under the condition of external constant disturbance, external constant disturbance is added to MLS in 5 s-5.2 s, the response of MLS in case of external constant disturbance is shown in Fig. 9.

According to Fig. 9, it can be observed that the anti-interference ability of Backstepping control is weakest in case of external constant disturbance. To be more specific, after adding disturbance, the overshoot of the proposed controller is 0.3668 mm, the overshoot of Backstepping control is 1.999 mm, and the overshoot of SMC is 0.5739 mm. Compared with SMC and Backstepping control, the overshoot of the proposed controller is the smallest. This result shows that the proposed controller has stronger anti-interference ability and faster convergence compared with Backstepping control and SMC.

In order to assess the robustness of the proposed controller, considering the mass of MLS changes slowly over time, the response of MLS in the presence of mass change is shown in Fig. 10 and Fig. 11, the performance analysis of the three controllers is given in table 5. From Fig. 10,

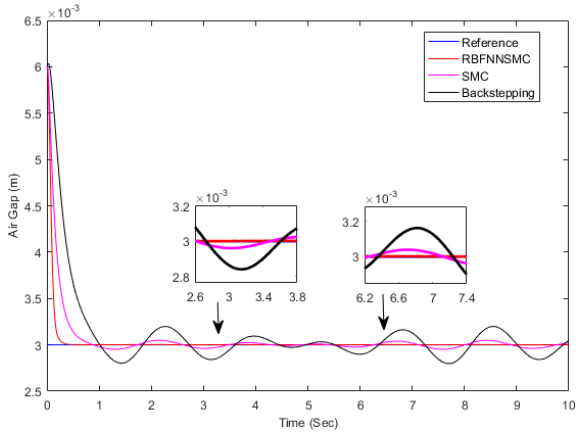

FIGURE 10. Tracking performance of RBFNNSMC, SMC and Backstepping control under the condition of mass change.

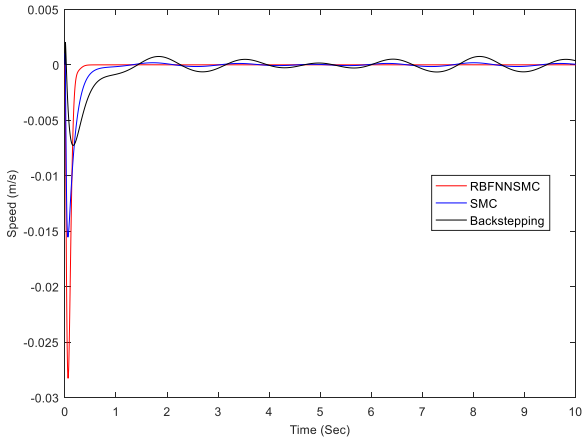

FIGURE 11. Tracking of Speed ($\dot{x}_1$) for RBFNNSMC, SMC and Backstepping control in the presence of mass change.

TABLE 5. Performance analysis of three controllers (mass change).

Index	RBFNNSMC	Sliding-Mode Control	Backstepping Control
Fluctuation	little	middle	large
Robustness	strong	middle	weak
Response speed	quick	middle	slow

Fig. 11, and table 5, the response of Backstepping control has the largest fluctuation in the presence of mass change. To be more specific, the response of Backstepping control fluctuates between 2.79 mm and 3.19 mm, if the parameter changes increases further, MLS maybe become unstable. the response of SMC fluctuates between 2.95 mm and 3.05 mm, the fluctuation of proposed controller's response is almost zero. The proposed controller uses neural networks to approximate unknown dynamics, so the influence of parameter changes on the system is extreme small. On the ground of analysis, we can see that proposed controller has better robustness compared with SMC and Backstepping control under the condition of mass change.

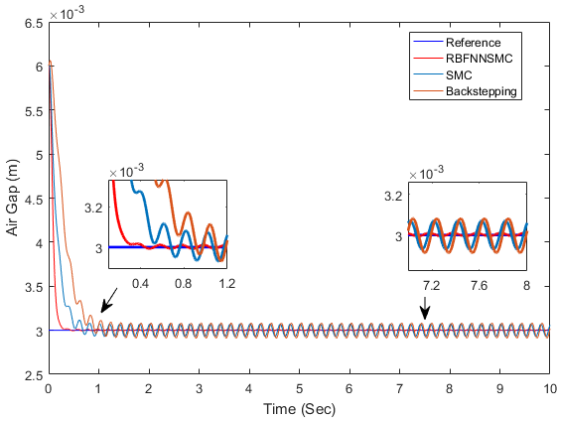

FIGURE 12. Tracking performance of RBFNNSMC, SMC and Backstepping control under the effect of unmodeled dynamic.

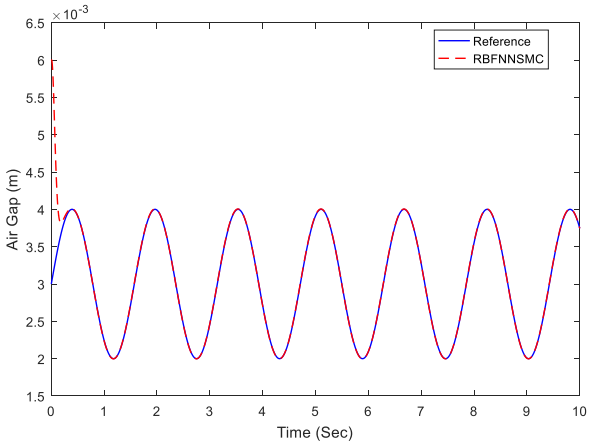

FIGURE 13. Tracking performance of RBFNNSMC with sinusoid input.

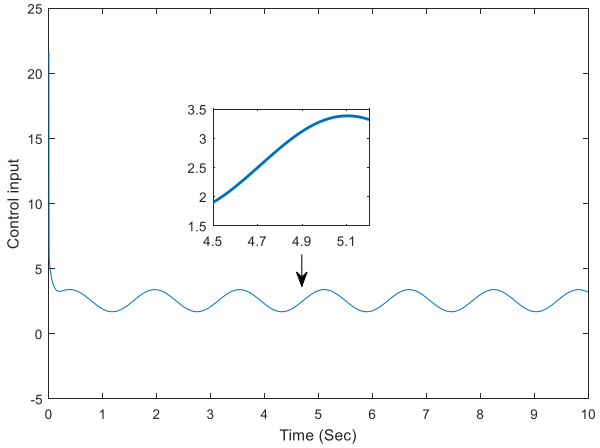

FIGURE 14. Control input with sinusoid input.

In addition to the problems of disturbance and parameter change during the operation of MLS, the unmodeled dynamics of MLS should be taken into consideration. It is assumed that there is the high frequency unmodeled dynamic ($0.3\sin(10\pi t)$) is added to MLS, the response of MLS in case of unmodeled dynamic is shown in Fig. 12. From Fig. 12, it can be seen clearly that all three controllers can make MLS run stably in the presence of unmodeled dynamic. More specifically, the response of SMC and Backstepping control has larger chattering than the proposed controller, if unmodeled dynamic increases further, SMC and Backstepping control maybe make MLS unstable. In term of analysis, we can see that the proposed controller has better effect on handling with unmodeled dynamic compared with SMC and Backstepping control.

The simulation of the proposed controller tracking sinusoidal signal will be given following. The reference input is given as $x_r = 0.003 + 0.001\sin(4t)$.

When selecting the reference input, the physical meaning should be considered, instead of blindly selecting the complex nonlinear reference input. As shown in Fig. 13, the proposed controller tracks the reference input nicely. According to Fig.14, there is no obvious chattering in the control input. The result shows that the proposed controller can nicely track the sinusoid input.

VI. CONCLUSION

In this paper, RBFNNSMC has been addressed for tracking problem of MLS with unknown dynamics. The unknown dynamics of MLS is approximated by RBFNN. The proposed controller guarantees that the closed-loop MLS is UUB. Simulation results have shown that the proposed controller has faster convergence and stronger robustness compared with SMC and Backstepping control. Due to the problem of parameters selection in the process of controller design, the intelligent optimization algorithm will be considered in the future research to optimize parameters.

REFERENCES

[1] Z.-J. Yang and M. Tateishi, "Adaptive robust nonlinear control of a magnetic levitation system," *Automatica*, vol. 37, no. 7, pp. 1125–1131, Jul. 2001.

[2] M. Zhai, Z. Long, and X. Li, "Fault-tolerant control of magnetic levitation system based on state observer in high speed Maglev train," *IEEE Access*, vol. 7, pp. 31624–31633, 2019, doi: 10.1109/ACCESS.2019.2898108.

[3] H. Wang, Z. Deng, S. Ma, R. Sun, H. Li, and J. Li, "Dynamic simulation of the HTS Maglev vehicle-bridge coupled system based on levitation force experiment," *IEEE Trans. Appl. Supercond.*, vol. 29, no. 5, pp. 1–6, Aug. 2019.

[4] S. Ganguly, M. K. Bera, and P. Roy, "Robust tracking and model following controller based on higher order sliding mode control and observation: With an application to MagLev system," 2020, *arXiv:2007.05750*. [Online]. Available: http://arxiv.org/abs/2007.05750

[5] I. Iswanto and A. Ma'arif, "Robust integral state feedback using coefficient diagram in magnetic levitation system," *IEEE Access*, vol. 8, pp. 57003–57011, 2020, doi: 10.1109/ACCESS.2020.2981840.

[6] Y. He, X. He, J. Ma, and Y. Fang, "Optimization research on a switching power amplifier and a current control strategy of active magnetic bearing," *IEEE Access*, vol. 8, pp. 34833–34841, 2020.

[7] H.-W. Lee, K.-C. Kim, and J. Lee, "Review of Maglev train technologies," *IEEE Trans. Magn.*, vol. 42, no. 7, pp. 1917–1925, Jul. 2006.

[8] Y. D. Chung, C. Y. Lee, D. W. Kim, H. Kang, Y. G. Park, and Y. S. Yoon, "Conceptual design and operating characteristics of multi-resonance antennas in the wireless power charging system for superconducting MAGLEV train," *IEEE Trans. Appl. Supercond.*, vol. 27, no. 4, pp. 1–5, Jun. 2017, doi: 10.1109/TASC.2017.2662233.

[9] X. Zhou, P. Wang, and Z. Long, "Fault detection for suspension system of Maglev trains based on historical health data," *IEEE Access*, vol. 8, pp. 134290–134302, 2020.
[10] G. Ahmad and U. Amin, "Design, construction and study of small scale vertical axis wind turbine based on a magnetically levitated axial flux permanent magnet generator," *Renew. Energy*, vol. 101, pp. 286–292, Feb. 2017.
[11] Z.-M. Li, X.-H. Chang, and J. H. Park, "Quantized static output feedback fuzzy tracking control for discrete-time nonlinear networked systems with asynchronous event-triggered constraints," *IEEE Trans. Syst., Man, Cybern. Syst.*, early access, Aug. 15, 2019, doi: 10.1109/TSMC.2019.2931530.
[12] J. Cai, R. Yu, B. Wang, C. Mei, and L. Shen, "Decentralized event-triggered control for interconnected systems with unknown disturbances," *J. Franklin Inst.*, vol. 357, no. 3, pp. 1494–1515, Feb. 2020.
[13] L. Ma, N. Xu, X. Huo, and X. Zhao, "Adaptive finite-time output-feedback control design for switched pure-feedback nonlinear systems with average dwell time," *Nonlinear Anal., Hybrid Syst.*, vol. 37, Aug. 2020, Art. no. 100908.
[14] Y. Chang, Y. Wang, F. E. Alsaadi, and G. Zong, "Adaptive fuzzy output-feedback tracking control for switched stochastic pure-feedback nonlinear systems," *Int. J. Adapt. Control Signal Process.*, vol. 33, no. 10, pp. 1567–1582, 2019.
[15] Z.-M. Li and J. H. Park, "Dissipative fuzzy tracking control for nonlinear networked systems with quantization," *IEEE Trans. Syst., Man, Cybern. Syst.*, early access, Sep. 24, 2018, doi: 10.1109/TSMC.2018.2866996.
[16] R. Morales, V. Feliu, and H. Sira-Ramirez, "Nonlinear control for magnetic levitation systems based on fast online algebraic identification of the input gain," *IEEE Trans. Control Syst. Technol.*, vol. 19, no. 4, pp. 757–771, Jul. 2011.
[17] J. Yang, A. Zolotas, W.-H. Chen, K. Michail, and S. Li, "Robust control of nonlinear MAGLEV suspension system with mismatched uncertainties via DOBC approach," *ISA Trans.*, vol. 50, no. 3, pp. 389–396, Jul. 2011.
[18] W.-Q. Zhang, J. Li, K. Zhang, and P. Cui, "Measurement and control of magnetic flux signal in a Maglev system," *Asian J. Control*, vol. 17, no. 1, pp. 165–175, Jan. 2015.
[19] Y. Zhang, B. Xian, and S. Ma, "Continuous robust tracking control for magnetic levitation system with unidirectional input constraint," *IEEE Trans. Ind. Electron.*, vol. 62, no. 9, pp. 5971–5980, Sep. 2015.
[20] A. Mughees and S. A. Mohsin, "Design and control of magnetic levitation system by optimizing fractional order PID controller using ant colony optimization algorithm," *IEEE Access*, vol. 8, pp. 116704–116723, 2020.
[21] A. S. Malik, I. Ahmad, A. U. Rahman, and Y. Islam, "Integral backstepping and synergetic control of magnetic levitation system," *IEEE Access*, vol. 7, pp. 173230–173239, 2019.
[22] A. A. Bobtsov, A. A. Pyrkin, R. S. Ortega, and A. A. Vedyakov, "A state observer for sensorless control of magnetic levitation systems," *Automatica*, vol. 97, pp. 263–270, Nov. 2018.
[23] H. M. M. Adil, S. Ahmed, and I. Ahmad, "Control of MagLev system using supertwisting and integral backstepping sliding mode algorithm," *IEEE Access*, vol. 8, pp. 51352–51362, 2020.
[24] A. R. Barron, "Universal approximation bounds for superpositions of a sigmoidal function," *IEEE Trans. Inf. Theory*, vol. 39, no. 3, pp. 930–945, May 1993.
[25] H. Yang and J. Liu, "An adaptive RBF neural network control method for a class of nonlinear systems," *IEEE/CAA J. Automatica Sinica*, vol. 5, no. 2, pp. 457–462, Mar. 2018.
[26] V. T. Yen, W. Y. Nan, and P. Van Cuong, "Recurrent fuzzy wavelet neural networks based on robust adaptive sliding mode control for industrial robot manipulators," *Neural Comput. Appl.*, vol. 31, no. 11, pp. 6945–6958, Nov. 2019.
[27] S. Huang and K. K. Tan, "Intelligent friction modeling and compensation using neural network approximations," *IEEE Trans. Ind. Electron.*, vol. 59, no. 8, pp. 3342–3349, Aug. 2012.
[28] Z. Chen, F. Huang, W. Sun, J. Gu, and B. Yao, "RBF-neural-network-based adaptive robust control for nonlinear bilateral teleoperation manipulators with uncertainty and time delay," *IEEE/ASME Trans. Mechatronics*, vol. 25, no. 2, pp. 906–918, Apr. 2020.
[29] C. Yang, G. Peng, L. Cheng, J. Na, and Z. Li, "Force sensorless admittance control for teleoperation of uncertain robot manipulator using neural networks," *IEEE Trans. Syst., Man, Cybern. Syst.*, early access, Jun. 28, 2019, doi: 10.1109/TSMC.2019.2920870.
[30] W. Yang, F. Meng, M. Sun, and K. Liu, "Passivity-based control design for magnetic levitation system," *Appl. Sci.*, vol. 10, no. 7, p. 2392, Apr. 2020.
[31] P. K. Sinha and A. N. Pechev, "Nonlinear H_∞ controllers for electromagnetic suspension systems," *IEEE Trans. Autom. Control*, vol. 49, no. 4, pp. 563–568, Apr. 2004.
[32] Y. Shtessel, C. Edwards, L. Fridman, and A. Levant, *Sliding Mode Control and Observation*. New York, NY, USA: Birkhaüser, 2014.
[33] D. Xue and Y. Chen, *System Simulation Techniques With MATLAB and Simulink*. Hoboken, NJ, USA: Wiley, 2013.
[34] D. Xue, *Calculus Problem Solutions With MATLAB*. Berlin, Germany: De Gruyter, 2020.

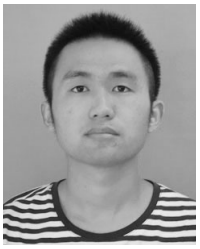

WANG YANG received the B.S. degree in automation specialty from the Heilongjiang University of Science and Technology, Harbin, China, in 2018. He is currently pursuing the M.S. degree with Northeastern University at Qinhuangdao, Qinhuangdao, China.

His current research interests include adaptive control and intelligent control.

FANWEI MENG received the B.S. degree in automation specialty from Harbin Engineering University, Harbin, China, in 2005, and the Ph.D. degree in control science and engineering from the Harbin Institute of Technology, Harbin, in 2013.

From 2005 to 2013, he was a Naval Technical Officer. Since 2014, he has been a Lecturer with the Control Science and Engineering Department, Northeastern University at Qinhuangdao, China. He is the author of one book and more than 20 articles. His research interests include robust control and control system design.

SHENGYA MENG is currently pursuing the master's degree with Northeastern University at Qinhuangdao, Qinhuangdao, Hebei, China.

She also works with Fanwei Meng as a Student Researcher. Her current research interest includes automatic control.

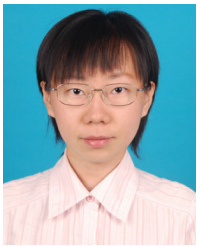

SUN MAN received the M.S. degree from Yanshan University, Qinhuangdao, China, in 2004, and the Ph.D. degree from Beihang University, Beijing, China, in 2009.

His research interests include robust control and time-delay systems.

AIPING PANG received the M.S. degree in mathematics from the College of Science, Harbin Institute of Technology, China, in 2013, and the Ph.D. degree in control science and engineering from the College of Aerospace, Harbin Institute of Technology, in 2018.

She is currently an Associate Professor with the Department of Automation, School of Electrical Engineering, Guizhou University, Guiyang, China. Her research interests include robot control, H-inf control, delay system control, spacecraft control.